

A mutation in the RCC1-related protein *pim1* results in nuclear envelope fragmentation in fission yeast

JANOS DEMETER*, MARY MORPHEW†, AND SHELLEY SAZER*‡§

*Verna and Marrs McLean Department of Biochemistry and †Department of Cell Biology, Baylor College of Medicine, One Baylor Plaza, Houston, TX 77030; and ‡Department of Molecular, Cellular, and Developmental Biology, University of Colorado, Boulder, CO 80309

Communicated by Salih J. Wakil, Baylor College of Medicine, Houston, TX, November 21, 1994 (received for review September 20, 1994)

ABSTRACT Members of the RCC1 protein family are chromatin-associated guanine nucleotide exchange factors that have been implicated in diverse cellular processes in various organisms, yet no consensus has been reached as to their primary biological role. The fission yeast *Schizosaccharomyces pombe*, a single-celled eukaryote, provides an *in vivo* system in which to study the RCC1/Ran switch by using a temperature-sensitive mutant in the RCC1-related protein *pim1*. Mitotic entry in the *pim1-d1^{ts}* mutant is normal, but mitotic exit leads to the accumulation of cells arrested with a medial septum and condensed chromosomes. Although the yeast nuclear envelope normally remains intact throughout the cell cycle, we found a striking fragmentation of the nuclear envelope in the *pim1-d1^{ts}* mutant following mitosis. This resulted in chromatin that was no longer compartmentalized and an accumulation of pore-containing membranes in the cytoplasm. The development of this terminal phenotype was dependent on the passage of cells through mitosis and was coincident with the loss of viability. We propose that *pim1* is required for the reestablishment of nuclear structure following mitosis in fission yeast.

RCC1 and Ran are human proteins forming the core of an evolutionarily conserved GTPase molecular switch: RCC1 is a chromatin-associated nucleotide exchange factor that interacts with the small GTPase Ran. This switch has been studied in a number of different organisms and has been implicated in a variety of cellular processes including chromatin conformation, nucleolar structure, chromosome stability, cell cycle progression, RNA processing, RNA export from the nucleus, protein import to the nucleus, and mating in budding yeast (reviewed in ref. 1; refs. 2–6). No consensus has been reached on the primary biological role of this GTPase switch.

The *pim1* protein (2, 6) of the fission yeast *Schizosaccharomyces pombe* is a structural homologue of RCC1 and *sp1* is nearly identical to human Ran. The *pim1* gene was cloned by complementation of temperature-sensitive lethal mutations in the *pim1* gene, and *sp1* was cloned as a high-copy suppressor of these mutations (2, 6). When fission yeast cells enter mitosis they activate the *p34^{cdc2}* protein kinase, condense their chromosomes, depolymerize their cytoplasmic microtubules, and organize a mitotic spindle within the nucleus, because unlike the nuclear membrane in multicellular eukaryotes, the nuclear envelope does not break down at mitosis in fission yeast (7). At the exit from mitosis the *p34^{cdc2}* kinase is inactivated, the chromosomes decondense, the mitotic spindle is depolymerized, and the cytoplasmic microtubules are reformed.

The fission yeast *pim1-d1^{ts}* mutant is unable to properly reestablish the interphase state following mitosis. At the restrictive temperature the cells activate the *p34^{cdc2}* protein kinase and enter mitosis with normal kinetics. After mitosis the cells inactivate *p34^{cdc2}* and form a medial septum but fail

to decondense their chromosomes (2). The terminal phenotype of the *pim1-d1* mutant led to the proposal that the *pim1* protein is required for the reestablishment of the interphase state following mitosis (2).

We now show that the *pim1-d1^{ts}* mutant undergoes nuclear envelope fragmentation at the restrictive temperature, a phenotype that is particularly striking in this organism, which does not undergo nuclear envelope breakdown at mitosis (7). We also show that the development of the *pim1-d1^{ts}* terminal phenotype is dependent on the passage of cells through mitosis and that the temperature-sensitive lethality occurs after the completion of mitosis. The lack of nuclear envelope integrity in this mutant may be the result of the inability to establish the interphase nuclear architecture following mitosis.

MATERIALS AND METHODS

Cell Culture. Wild-type 972h– and mutant *pim1-d1^{ts}* cells (2) were grown by standard procedures (8). For electron microscopy, *pim1-d1^{ts}* cells in early logarithmic phase were incubated at either 25°C or 36°C for 4 hr. For all other experiments, *pim1-d1^{ts}* cells were synchronized in the G₂ stage of the cell cycle by centrifugal elutriation with a Beckman model JE-5.0 rotor and then incubated at either 25°C or 36°C. Cell cycle progression was monitored by counting the percentage of septated cells. Chromosome condensation was monitored by 4',6-diamidino-2-phenylindole (DAPI) staining of formaldehyde-fixed cells (8). Nuclear envelope abnormalities were monitored by staining live cells with 3,3'-dihexyloxycarbocyanine iodide (DiOC₆). Viability was assayed by removing 150 μl of cells, diluting them in 10 ml of room-temperature medium, briefly sonicating, and then plating in quadruplicate. Colony number was counted after 3 days at 25°C and the four numbers were averaged. Cell number was determined with a Coulter Counter. Viability was calculated as average colony number per cell number plated. *pim1-d1^{ts}* cells from a synchronous culture were treated with 12 mM hydroxyurea just prior to the peak of septation at 25°C to block DNA replication and then shifted to 36°C just after the peak of septation, as previously described (2), and observed 4 hr later. Benomyl was used to prevent mitosis (9). *pim1-d1^{ts}* cells in midlogarithmic phase were treated with benomyl (7.2 μg/ml) for 4 hr at 25°C and then shifted to 36°C for 4 hr.

Microscopy. Membrane staining. Cells were synchronized by centrifugal elutriation to enrich for mitotic cells. The lipophilic dye DiOC₆ (5 μg/ml) and the DNA-binding dye Hoechst 33342 (50 μg/ml) were added to growing cells (10). Live cells were observed with a Zeiss Axioskop fluorescence microscope.

Nuclear pore staining. Cells were fixed in methanol/formaldehyde (11) for 30 min and then processed for immunofluorescence by the protocol of Hagan and Hyams (12) with minor modifications: cell wall digestion was performed with

The publication costs of this article were defrayed in part by page charge payment. This article must therefore be hereby marked "advertisement" in accordance with 18 U.S.C. §1734 solely to indicate this fact.

Abbreviations: DAPI, 4',6-diamidino-2-phenylindole; DiOC₆, 3,3'-dihexyloxycarbocyanine iodide.

§To whom reprint requests should be addressed.

Novozyme (0.7 mg/ml) and Zymolyase (0.2 mg/ml) for 5 min at 20°C. The primary antibody, raised to rat liver nuclear proteins; (MAb414; BabCo, Emeryville, CA), was applied overnight at 4°C, undiluted; the secondary antibody (Texas Red-conjugated donkey anti-mouse; Jackson ImmunoResearch) was used at 1:100 dilution for 1 hr at 20°C. Cells were mounted and stained with the DNA-binding dye DAPI (12). Cells were observed and photographed with a Zeiss Axioskop fluorescence microscope.

Electron microscopy. The cells were collected on a 0.45- μ m Millipore filter by vacuum filtration and were frozen in a Balzers high-pressure freezer. Frozen samples for conventional electron microscopy were freeze-substituted by a modification of the method of Ding *et al.* (13). Samples were substituted into 0.1% tannic acid in acetone at -90°C for 2 days, rinsed in acetone at this temperature, and placed in 1% OsO₄ in acetone at -90°C for 2 days. Samples were then warmed to room temperature over 24 hr, rinsed in acetone, and embedded in Epon/Araldite. Sections (80 nm) were cut with a Reichert model Ultracut E microtome and picked up on formvar-coated, carbon-stabilized slot grids. For immunoelectron microscopy, frozen samples were fixed and dehydrated in acetone containing 0.1% glutaraldehyde for 4 days at -90°C (14). Cells were warmed to 0°C over 24 hr, rinsed in cold acetone, embedded in L.R. White resin (London Resin, Hampshire, England), and polymerized under vacuum at 45°C. Sections were cut and picked up as described above and then

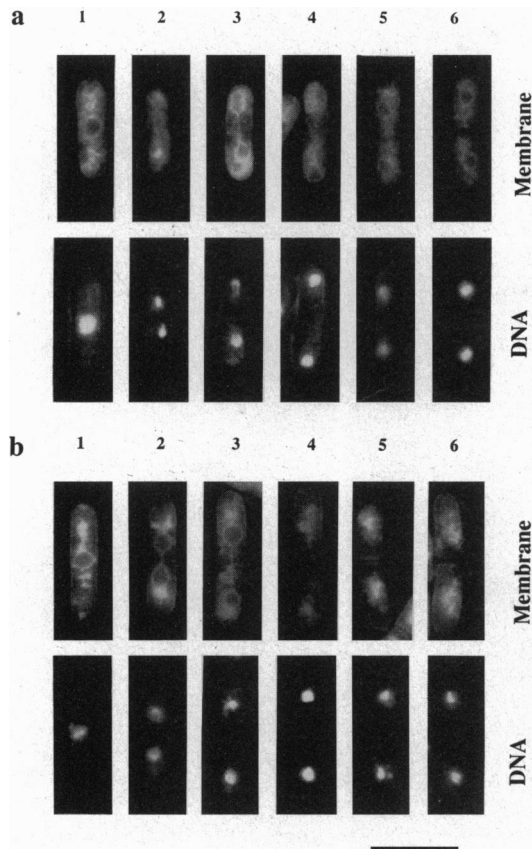


FIG. 1. Intracellular membrane organization is altered in *pim1-d1^{ts}* arrested cells. Synchronized *pim1-d1^{ts}* cells in mitosis were double stained with the vital general membrane stain DiOC₆ and the vital DNA stain Hoechst 33342. Micrographs of mitotic cells grown at the permissive temperature (25°C) (*a*) and the restrictive temperature (36°C) (*b*) were arranged according to position in mitosis. During mitosis (*a* 1-3 and *b* 1-3) the nuclear envelope staining followed the same pattern at 25°C and 36°C, but after cytokinesis the nuclei became smaller (compare *a* 4 and *b* 4) and eventually the membrane staining was not detectable (*b*5). (Bar = 10 μ m.)

stained with BWD-1 antibodies to DNA (15) (kindly provided by Brian Kotzin, National Jewish Center for Immunology and Respiratory Medicine, Denver) or with MAb414 antibodies to the nuclear pore complex, followed by secondary antibodies conjugated to 10-nm gold particles (Biocell Laboratories) (16). Sections were poststained with uranyl acetate and lead citrate and imaged in a Philips CM10 electron microscope operating at 80 kV.

RESULTS

Nuclear Envelope Is Abnormal in *pim1-d1^{ts}* Arrested Cells. The fission yeast *Sch. pombe* undergoes a "closed" mitosis in which the nuclear envelope does not break down, as it does in higher eukaryotes (7). At all stages of the cell cycle the lipophilic dye DiOC₆ surrounded the DNA and localized to the nuclear periphery in wild-type cells (data not shown) and in *pim1-d1^{ts}* cells grown at the permissive temperature (Fig. 1*a*).

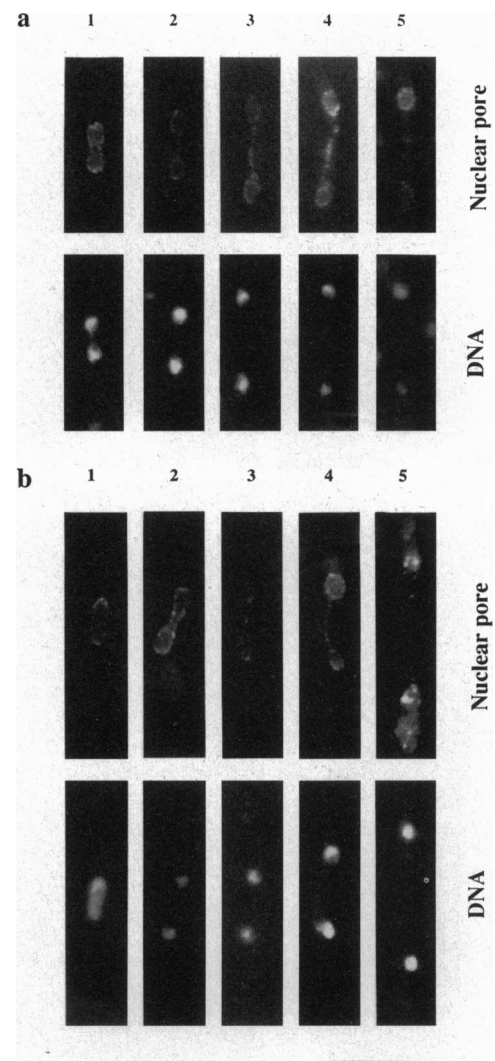


FIG. 2. Nuclear pore complex localization is altered in *pim1-d1^{ts}* arrested cells. *pim1-d1^{ts}* cells were immunostained with the anti-nuclear pore complex antibody MAb414 and the fluorescent DNA stain DAPI. (*a*) *pim1-d1^{ts}* cells at the permissive temperature in different stages of mitosis. The nuclear pore staining delineated the nuclear envelope in a pattern similar to that of DiOC₆. (*b*) *pim1-d1^{ts}* cells went through mitosis at 36°C with their nuclear membrane intact (*b* 1-4), repeating the pattern observed at 25°C (*a* 1-4). After cytokinesis (*b*5), the DNA became hypercondensed, the nuclear envelope lost its integrity, and nuclear pore staining appeared in the cytoplasm. (Bar = 10 μ m.)

When incubated at the restrictive temperature, *pim1-d1^{ts}* cells showed a normal DiOC₆ pattern until mitosis was completed (Fig. 1 *b 1-4*), and after cytokinesis the nuclei became smaller (Fig. 1 *b 4*). Thereafter the nuclear periphery was no longer evident (Fig. 1 *b 5* and 6). We saw the same pattern of DiOC₆ staining in strains carrying two different temperature-sensitive mutations in *pim1*, one of which is identical to *pim1-46* (6) (J.D. and S.S., unpublished data). However, since this dye is not specific for the nuclear envelope, these observations did not allow us to determine whether the nuclear envelope was absent or obscured by cytoplasmic membrane.

Distribution of Nuclear Pores Is Abnormal in *pim1-d1^{ts}* Arrested Cells. The nuclear envelope can be visualized more specifically by monitoring the location of the nuclear pores. Several monoclonal antibodies raised to rat liver nuclear proteins react with the nuclear pore complex in both mammalian cells and budding yeast with a characteristic patchy immuno-

fluorescence staining pattern at the nuclear periphery (11, 17-20). This same pattern was seen in fission yeast stained with two of these antibodies, the monoclonal antibodies MAb414 (Fig. 2*a*) and MAb350 (data not shown). We tested MAb414 by immunoelectron microscopy and found that it localized preferentially to the nuclear pore complex (see Fig. 3*c* below) and could be used as a marker to follow the fate of the nuclear envelope in fission yeast.

During all stages of mitosis in *pim1-d1^{ts}* cells at the permissive temperature, the nuclear pores were relatively uniformly distributed in the nuclear envelope and completely surrounded the DAPI-staining chromatin region (Fig. 2 *a 1-5*). At the restrictive temperature the distribution of nuclear pores remained the same in interphase and mitosis (Fig. 2 *b 1-4*), but after mitosis the pattern changed (compare Fig. 2 *a 5* and 2 *b 5*). The phenotypes observed are illustrated in the septated cell shown in Fig. 2 *b 5*. In the top half of this cell, the pores no

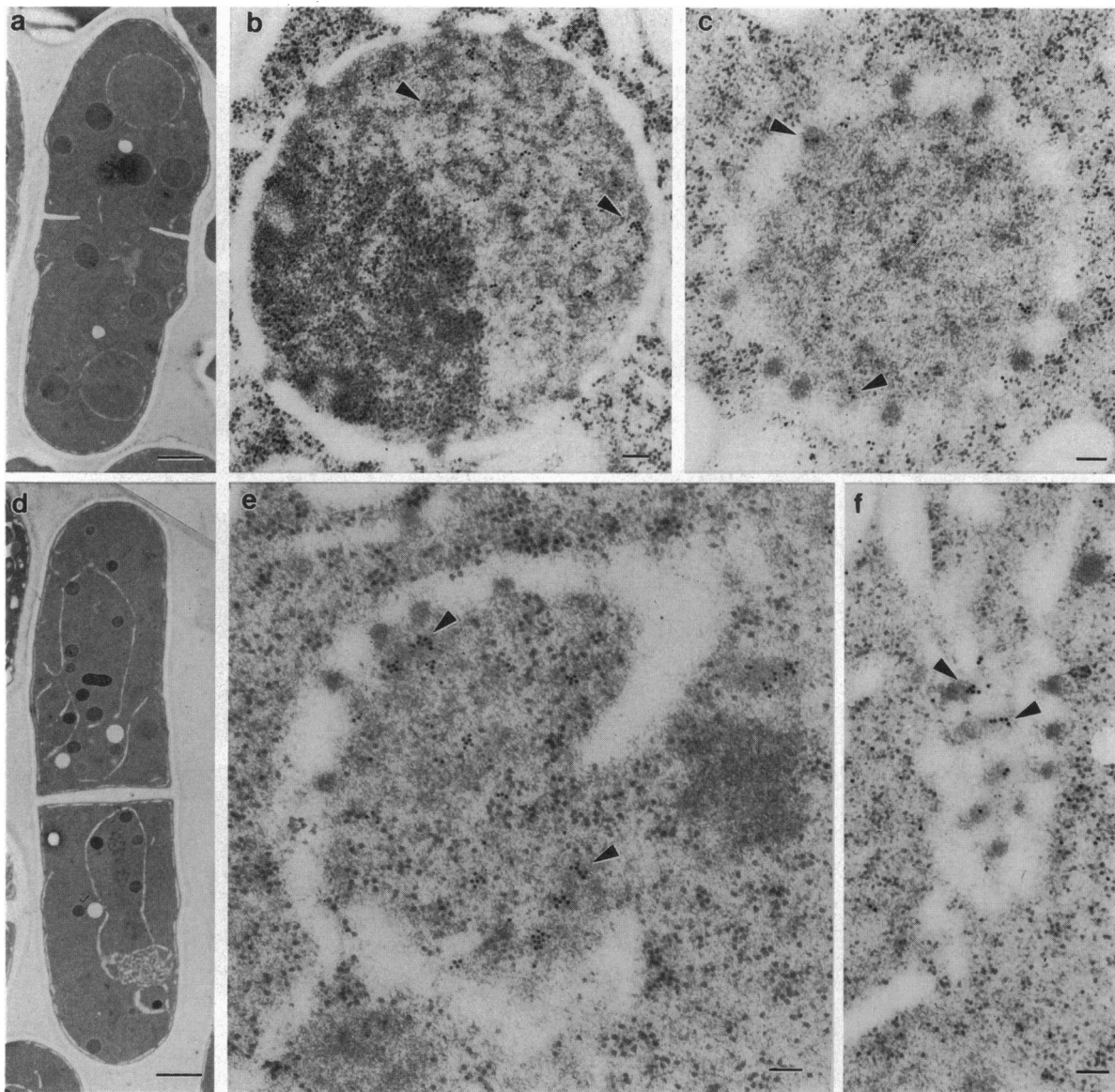


FIG. 3. Nuclear envelope is fragmented in *pim1-d1^{ts}* arrested cells. (*a* and *d*) Electron micrographs of *pim1-d1^{ts}* cells at the permissive (*a*) and restrictive (*d*) temperatures. At 25°C cells had nuclei with normal morphology: a circular double membrane decorated with nuclear pores (*a*). At 36°C arrested cells, which could be identified by the presence of a wide medial septum, did not have an intact nuclear envelope and had nuclear pore and membrane aggregates in the cytosol (*d*). (*b*, *c*, *e*, and *f*) Immunoelectron micrographs of *pim1-d1^{ts}* cells at 25°C (*b* and *c*) or 36°C (*e* and *f*) stained with anti-DNA antibody BWD-1 (*b* and *e*) or anti-rat nuclear pore complex antibody MAb414 (*c* and *f*). At 25°C (*b*) the DNA localized to one half of the nucleus. At 36°C (*e*) the DNA was associated with nuclear membrane material, although the membrane was not intact. MAb414 localized to the nuclear pore (*c*), and immunoreactive material was also present in cytoplasmic membrane fragments (*f*). Bar = 1 μ m in *a* and *d* and 100 nm in *b*, *c*, *e*, *f*.

longer completely surround the chromatin, and in the bottom half there are discrete brightly staining regions in the cytoplasm, suggesting pore aggregation.

Nuclear Envelope Is Fragmented in *pim1-d1* Arrested Cells. Thin-section electron microscopy was used to determine the ultrastructural basis of this abnormal immunofluorescence pattern. *pim1-d1*^{ts} arrested cells, identified by the presence of a medial septum, showed a dramatic fragmentation of the nuclear envelope and an increase in cytoplasmic membranes (compare Fig. 3 *a* and *d*). Because fission yeast chromatin is indistinct in the electron microscope and nuclear pores could not be definitively identified in the membranes of arrested cells that did not have a typical nucleus, we followed their behavior by immunoelectron microscopy, illustrated by representative micrographs in Fig. 3 *b*, *c*, *e*, and *f*. The typical fission yeast nucleus was completely surrounded by a pore-containing nuclear envelope (Fig. 3 *a-c*) and the DNA was confined to one half of the nucleus (Figs. 1, 2, and 3*b*; ref. 21). In *pim1-d1*^{ts} arrested cells the nuclear membrane was fragmented (Fig. 3 *d* and *e*) but the DNA remained associated with some but not all of the pore-containing double membranes (Fig. 3*e*), presumably of nuclear origin. Aggregates of nuclear pores were also found in membranous material within the cytoplasm (Fig. 3*f*), probably corresponding to the cytoplasmic immunofluorescence signal seen with this antibody (Fig. 2 *b* 5).

***pim1-d1*^{ts} Cells Undergo Nuclear Envelope Fragmentation and Loss of Viability After Mitosis.** Nitrogen-starved *pim1-d1* cells released from G₁ at the restrictive temperature or spores germinated at the restrictive temperature replicate their DNA and enter mitosis, but then the postmitotic cells arrest with condensed chromosomes, a medial septum, and a 1C DNA content per nucleus (2). The same terminal phenotype is seen when cells from a synchronous culture are periodically shifted

from the permissive to the restrictive temperature, regardless of their position in the cycle at the time of the shift (data not shown). Sazer and Nurse (2) have proposed that after the nucleus is reorganized for mitosis, the *pim1* function is required to reestablish the interphase state. This hypothesis predicts that development of the lethal *pim1-d1*^{ts} terminal phenotype requires passage through mitosis. We tested this prediction in two ways. Mutant cells blocked in interphase were shifted to the restrictive temperature to determine whether they underwent the phenotypic changes associated with the *pim1-d1*^{ts} phenotype. The nuclear envelope did not become fragmented, the chromatin did not condense, and the viability remained high in cells incubated at the restrictive temperature while arrested in S phase by hydroxyurea (Fig. 4*a*) or in G₂ by benomyl (Fig. 4*b*). A synchronous culture of *pim1-d1*^{ts} cells (Fig. 4*c*) was incubated at the restrictive temperature to monitor development of the terminal phenotype (Fig. 4*c* and *d*) and cell viability (Fig. 4*e*). Septated cells with hypercondensed chromosomes accumulated at the restrictive temperature, coincident with the appearance of nuclear envelope abnormalities (Fig. 4*c* and *d*). Although the *pim1-d1*^{ts} cell cycle arrest is established rapidly and the chromosomes remain condensed throughout mitosis (2), cells retained viability at the restrictive temperature equal to that at the permissive temperature until the completion of mitosis and septation, then viability of cells at the restrictive temperature declined (Fig. 4*e*). These experiments demonstrate that the development of the *pim1-d1*^{ts} phenotype is dependent on the passage of cells through mitosis.

DISCUSSION

RCC1 and Ran influence a variety of cellular processes (reviewed in ref. 1), including mRNA export (22–24), protein

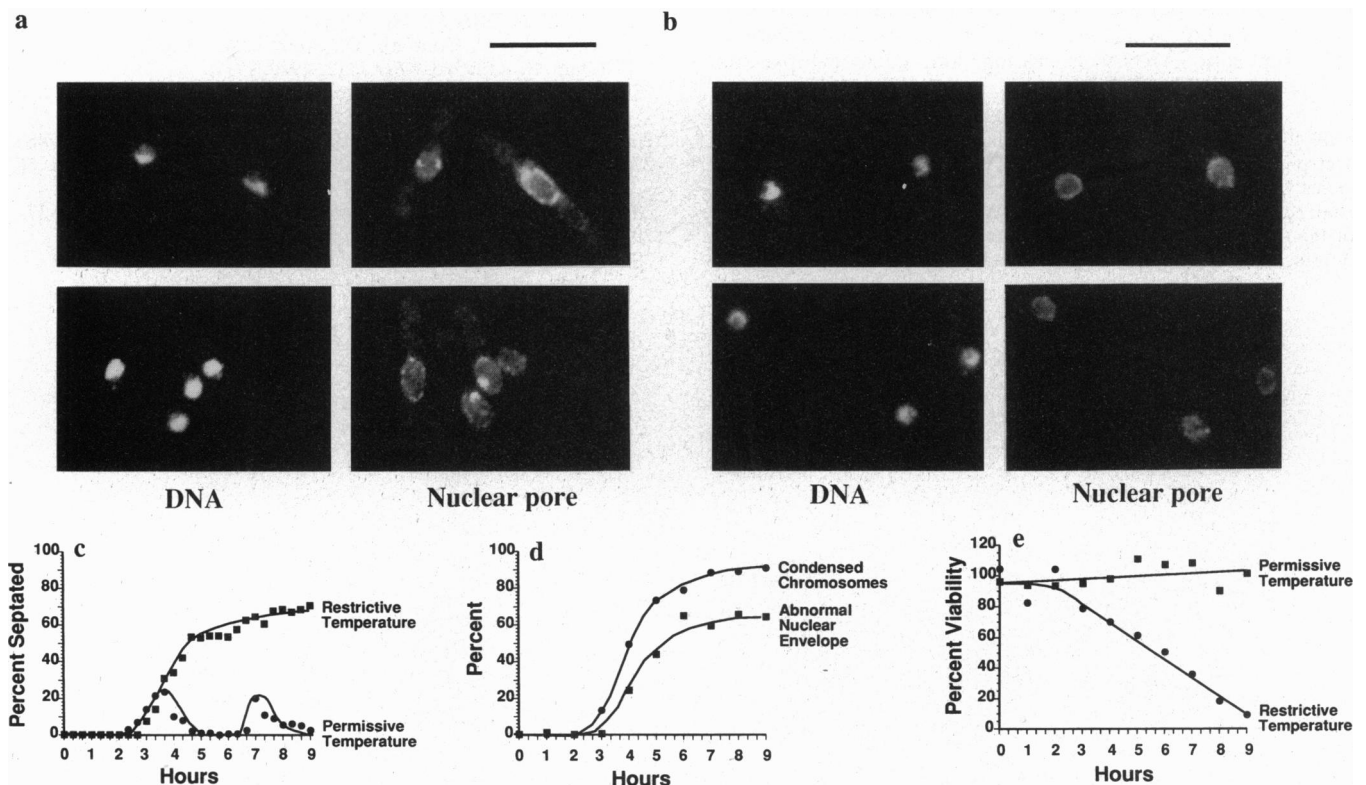


FIG. 4. *pim1-d1*^{ts} cells lose viability after mitosis. (*a* and *b*) *pim1-d1*^{ts} cells were arrested in interphase with either hydroxyurea (*a*) or benomyl (*b*), incubated at the restrictive temperature, and then stained with anti-nuclear pore antibody MAb414 and DAPI. Cells have decondensed chromatin and an intact nuclear envelope. (Bar = 10 μ m.) (*c-e*) A synchronous culture of *pim1-d1*^{ts} cells was prepared by centrifugal elutriation and incubated at either 25°C (permissive temperature) or 36°C (restrictive temperature). Percentage of septated cells (*c*), percentage of cells with condensed chromosomes or abnormal nuclear envelope (*d*), and relative percentage of viable cells (25°C sample at 0 hr defined 100% viability) (*e*).

import (3, 4), DNA replication (25, 26), cell cycle progression (2, 5, 26), and nuclear envelope growth and reformation (5, 25, 26). Based on these studies, numerous models have been proposed (1–5, 22–26) but no consensus has been reached on the primary role of RCC1/Ran or on whether this biological role is evolutionarily conserved. The high viability of *pim1-d1^{ts}* cells at the restrictive temperature until they pass through mitosis and the fact that these mutant cells enter mitosis with normal kinetics suggest that mRNAs encoding the mitotic control proteins *cdc2*, *cdc13* (cyclin B), and *cdc25* are synthesized, transported out of the nucleus, and translated and the proteins properly localized to the nucleus. Our data favor the view that the primary role of the RCC1/Ran complex in fission yeast is in the control of nuclear architecture and that some of the phenotypes associated with mutation or depletion of RCC1 and/or Ran in this and other systems may reflect their dependence on nuclear organization. In interphase fission yeast cells, the nuclear envelope, chromatin, DNA replication complexes, and RNA processing centers could be associated with as yet unidentified architectural elements of the nucleus, analogous to the nuclear matrix or nuclear lamina in other systems. At mitosis these associations would be expected to be disrupted in fission yeast as they are in multicellular eukaryotes (reviewed in refs. 27–30). The primary defect in the *pim1-d1^{ts}* mutant may be the failure to reestablish the interphase architecture in the nucleus following mitosis. This is consistent with our observation that the temperature-sensitive lethality is dependent on passage through mitosis.

pim1-d1^{ts} mutant cells arrest with condensed chromosomes, a fragmented nuclear envelope, and an unreplicated genome. This terminal phenotype is consistent with a defect in nuclear architecture that would affect a variety of cellular processes dependent on the proper structural organization of the nucleus. The manifestations of this defect, which may vary among organisms and experimental systems, include nuclear envelope growth and integrity, chromatin and nucleolar conformation, DNA replication, RNA processing, and nucleocytoplasmic transport.

We thank Richard McIntosh for discussions and for help with the electron microscopy, Susan Wentz for samples of monoclonal antibodies MAb414 and MAb350 used in early stages of this work, Dr. Brian Kotzin for anti-DNA antibody BWD-1, and Dr. L. A. Staehelin for the generous use of his high-pressure freezer. We thank Richard McIntosh, Kathy Gould, Julian Blow, and Sue Berget for comments on

the manuscript. This work was supported by grants from the Robert A. Welch foundation (Q-1226 to S.S.) and the National Institutes of Health (GM49119 to S.S. and RR00592 to J. R. McIntosh).

1. Dasso, M. (1993) *Trends Biochem.* **18**, 96–101.
2. Sazer, S. & Nurse, P. (1994) *EMBO J.* **13**, 606–615.
3. Moore, M. S. & Blobel, G. (1993) *Nature (London)* **365**, 661–663.
4. Melchior, F., Paschal, B., Evans, J. & Gerace, L. (1993) *J. Cell Biol.* **123**, 1649–1659.
5. Kornbluth, S., Dasso, M. & Newport, J. W. (1994) *J. Cell Biol.* **125**, 705–719.
6. Matsumoto, T. & Beach, D. (1991) *Cell* **66**, 347–360.
7. Heath, J. B. (1980) *Int. Rev. Cytol.* **64**, 1–80.
8. Moreno, S., Klar, A. & Nurse, P. (1991) *Methods Enzymol.* **194**, 795–823.
9. Fantes, P. A. (1982) *J. Cell Sci.* **55**, 383–402.
10. Koning, A. J., Lum, P. Y., Williams, J. M. & Wright, R. (1993) *Cell Motil. Cytoskeleton* **25**, 111–128.
11. Wentz, S. R., Rout, M. P. & Blobel, G. (1992) *J. Cell Biol.* **119**, 705–723.
12. Hagan, I. M. & Hyams, J. S. (1988) *J. Cell Sci.* **89**, 343–357.
13. Ding, B., Turgeon, R. & Parthasarathy, M. V. (1991) *J. Electron Microsc. Tech.* **19**, 107–117.
14. Dahl, R. & Staehelin, L. A. (1989) *J. Electron Microsc. Tech.* **13**, 165–174.
15. Kotzin, B., Lafferty, J. A., Portanova, J. P., Rubin, P. L. & Tan, E. M. (1984) *J. Immunol.* **133**, 2555–2569.
16. Kiss, J. Z. & McDonald, K. (1993) *Methods Cell Biol.* **37**, 311–341.
17. Davis, L. I. & Blobel, G. (1986) *Cell* **45**, 699–709.
18. Davis, L. I. & Blobel, G. (1987) *Proc. Natl. Acad. Sci. USA* **84**, 7552–7556.
19. Davis, L. I. & Fink, G. R. (1990) *Cell* **61**, 965–978.
20. Aris, J. P. & Blobel, G. (1989) *J. Cell Biol.* **108**, 2059–2067.
21. Toda, T., Yamamoto, M. & Yanagida, M. (1981) *J. Cell Sci.* **52**, 271–287.
22. Forester, W., Stutz, M., Rosbash, M. & Wickens, M. (1992) *Genes Dev.* **6**, 1914–1926.
23. Amberg, D. C., Fleishmann, M., Stagljar, I., Cole, C. N. & Aebi, M. (1993) *EMBO J.* **12**, 233–241.
24. Kadowaki, T., Goldfarb, D., Spitz, L. M., Tartakoff, A. M. & Ohno, M. (1993) *EMBO J.* **12**, 2929–2937.
25. Dasso, M., Nishitani, H., Kornbluth, S., Nishimoto, T. & Newport, J. W. (1992) *Mol. Cell Biol.* **12**, 3337–3345.
26. Nishimoto, T., Eilen, E. & Basilico, C. (1978) *Cell* **15**, 475–483.
27. Newport, J. W. & Forbes, D. J. (1987) *Annu. Rev. Biochem.* **56**, 535–565.
28. Gerace, L. & Burke, B. (1988) *Annu. Rev. Cell Biol.* **4**, 335–374.
29. Spector, D. L. (1993) *Annu. Rev. Cell Biol.* **9**, 265–315.
30. Hozak, P. & Cook, P. R. (1994) *Trends Cell Biol.* **4**, 48–52.